

PROCESS SIMULATION ON THE IBM PERSONAL COMPUTER

M. Koltai, S. Trutz*

Technical University Budapest
Egry J. u. 18, Budapest, Hungary, H-1111

Enterprise for Microelectronics*
Foti ut 56, Budapest, Hungary, H-1325

SUMMARY

Our user oriented process simulation program called APT (Advanced Program for Technology) has been implemented on the IBM personal computer and its compatibles. APT can simulate most up-to-date process steps in two-dimensions and even in three-dimensions for the diffusion and ion implantation steps [1]. APT has the unique capability among two dimensional process simulators to determine the impurity distribution in the whole Si-SiO₂ system. At local oxidation the oxide shape is calculated by a general solution procedure based on steady-state oxidant diffusion and viscous flow of the oxide elements. As an extra feature APT can also simulate layer etching and deposition. Physical models as well as numerical techniques are discussed in the paper. The power of APT is illustrated by numerous simulation results.

SOLUTION OF THE DIFFUSION EQUATION

The governing equations for the redistribution of impurities during local oxidation are as follows:

Diffusion equation in the silicon:

$$\frac{\partial C_{jSi}}{\partial t} = \text{div} (D_{jSi} \text{grad} C_{jSi}) \quad (1)$$

Diffusion equation in the oxide:

$$\frac{\partial C_{jox}}{\partial t} = \text{div} (D_{jox} \text{grad} C_{jox}) \quad (2)$$

Boundary condition on the Si-SiO₂ interface:

$$D_{jSi} \frac{\partial C_{jSi}}{\partial n} = v_n C_{jSi} (k - \alpha) + D_{jox} \frac{\partial C_{jox}}{\partial n} \quad (3)$$

On the symmetry axes:

$$\frac{\partial C_{jSi}}{\partial n} = 0, \quad \frac{\partial C_{jox}}{\partial n} = 0 \quad (4)$$

where:

k is the segregation coefficient, $k = C_{ox}/C_{Si}$

\bar{n} is the unit normal to the Si-SiO₂ interface

v_n is the oxid growth rate, normal to the interface

C_{jSi}, C_{jox} denote the concentration of the j -th impurity

D_{jSi}, D_{jox} are concentration dependent diffusivities

α is the amount of Si consumed to produce one unit of oxide (0.44)

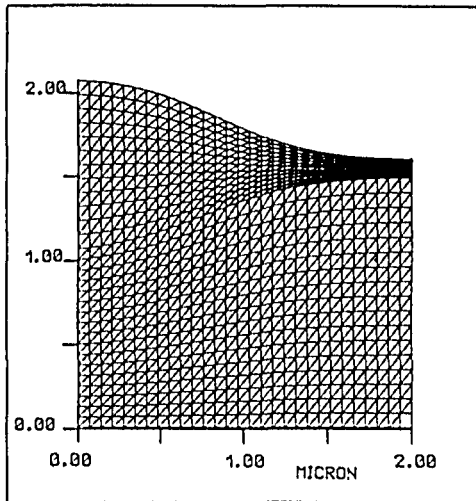


Fig. 1. Triangle mesh at local oxidation.

The governing equations are approximated as follows. Let's consider the triangle mesh in Fig. 1.

Assume $C(x,y)$ to be a linear function of position in each triangle. Then for a given triangle

$$\text{grad } C = \frac{(C_1 - C_0) \bar{s}_2^+ - (C_2 - C_0) \bar{s}_1^+}{\bar{s}_1 \bar{s}_2^+} \quad (5)$$

where:

C_0, C_1, C_2 denote the concentrations at the respective vertices

\bar{s}_1, \bar{s}_2 are the side vectors from C_0 to C_1 and C_0 to C_2 respectively. \bar{s}^+ represents the vector rotated clockwise by an angle $\pi/2$.

Using Gauss' theorem:

$$\int_V \text{div} (D \text{ grad } C) dV = \int_A D \text{ grad } C \bar{dA} \quad (6)$$

around the mesh points, the right hand side of the diffusion equations (1),(2) can be easily discretized. More details of this technique may be found in [16]. It can be shown that the resulting finite difference equations are identical to the finite element equations. Making use of (5) and

$$\frac{\partial C}{\partial n} = \bar{n} \text{ grad } C \quad (7)$$

the discretization of boundary conditions (3),(4) is straightforward. The moving boundary problem in local oxidation is solved through continuous grid deformation. As the oxidation is proceeding the grid is deformed step by step conforming to the oxide shape (see Fig. 1.) The total change of concentration is

$$\frac{dC}{dt} = \frac{\partial C}{\partial t} + \bar{v}_g \text{ grad } C \quad (8)$$

where \bar{v}_g is the velocity of the respective grid point [6].

Euler's implicit method has been used for time discretization of this equation.

The resulting linear matrix equations are solved by Stone's method [2]. Coupling and nonlinearities are treated in a similar way as in [4].

VERIFICATION

We checked our algorithm by comparing our numerical solution with some exact one dimensional analytic solutions [3], [5] and the coordinate transformation algorithm used in BICEPS [4]. There was a good agreement with less than 0.005 relative error, even on a very coarse 20x20 grid. The details of these tests are shown in Figs. 2 to 6.

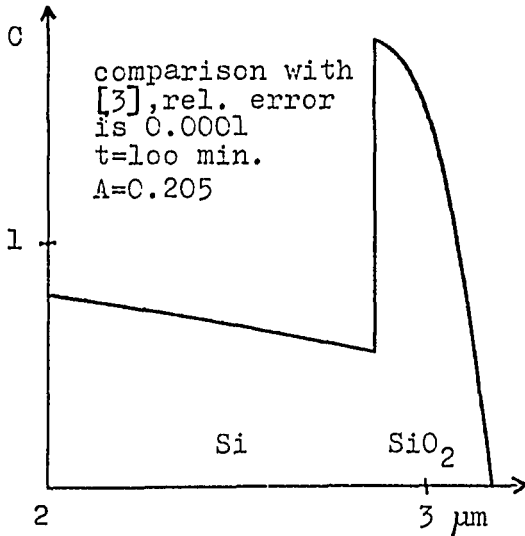


Fig. 2. Comparison with a 1D analytic solution obtained by Grove [3].

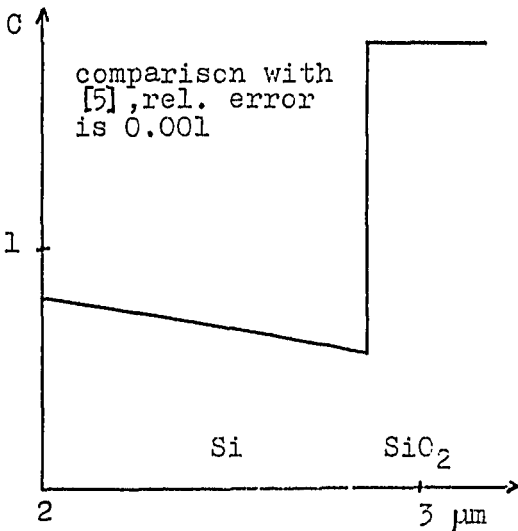


Fig. 3. Comparison with a 1D analytic solution obtained by Av-Ron [5].

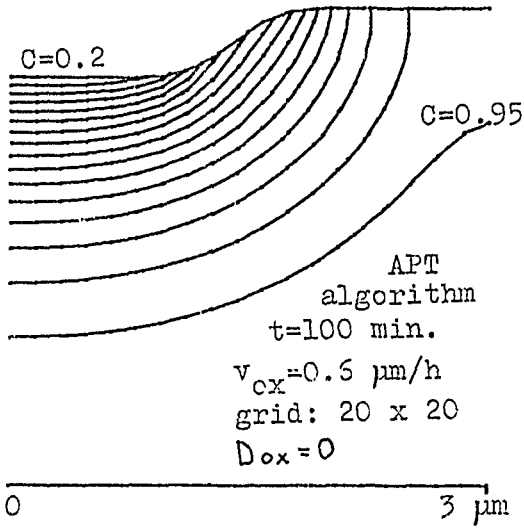


Fig. 4.
Equiconcentration lines obtained by APT algorithm.

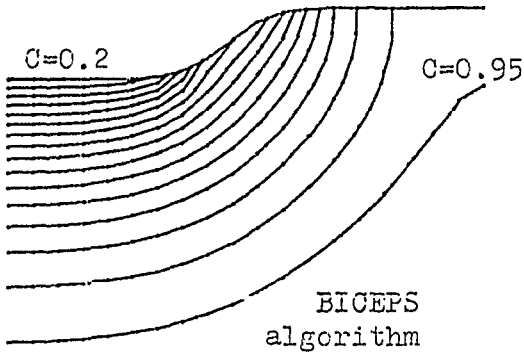


Fig. 5.
Equiconcentration lines obtained by BICEPS algorithm [4]

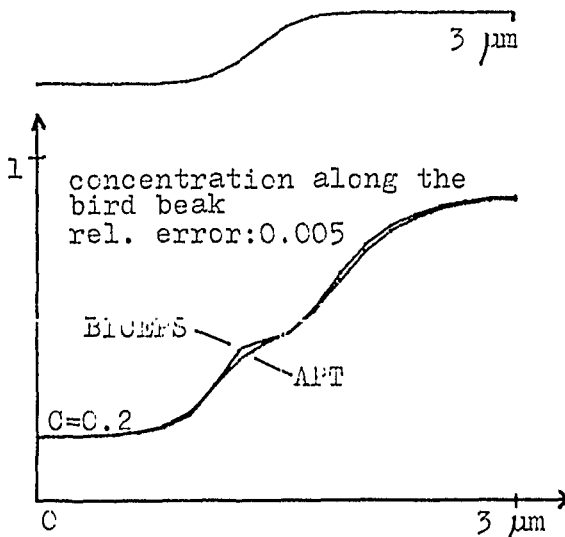


Fig. 6. Comparison of the algorithms of APT and BICEPS.

DIFFUSIVITY MODEL

The diffusion coefficient as a function of vacancy concentration is given by Fair [7],

$$D = D^x + D^+ \left(\frac{n_i}{n} \right) + D^- \left(\frac{n_-}{n_i} \right) + D^- \left(\frac{n_-}{n_i} \right)^2$$

APT takes into account the following secondary effects:

- OED
- excess vacancy concentration due to high phosphorous concentration [8].

OXIDATION MODEL

Our two-dimensional physical model is based on steady state oxygen diffusion and slow viscous flow of oxide. Similar models have already been described in literature [11],[12],[13]. However, our solution method is different. We apply the same grid deformation and approximation technique as for the determination of dopant concentration. This way the same grid can be used for the representation of dopant and oxidant concentration, as well as for the determination of the velocity and pressure distribution in the silicon dioxide.

The oxidant concentration is obtained by solving the steady state diffusion equation:

$$\text{div}(D_{ox} \text{ grad } C) = 0 \quad (9)$$

where D_{ox} is the oxidant diffusivity. The boundary conditions applied are:

On the Si-SiO₂ interface [11]

$$F = kC \quad (10)$$

where F is the oxidant flux normal to the interface, k is the oxidation reaction rate.

On the oxidant-oxide interface equilibrium oxidant concentration is assumed.

The velocity and pressure distribution of the oxide elements are obtained from the steady Navier-Stokes equations:

$$\text{div grad } \bar{V} = \text{grad } P \quad (11)$$

$$\text{div } \bar{V} = 0 \quad (12)$$

where μ is the viscosity, \bar{V} is the velocity, P is the pressure of the oxide elements [11].

On the Si-SiO₂ interface the velocity of the oxide elements is fixed [11],[13]:

$$V = - (1 - \alpha) \frac{kC}{N_1} \quad (13)$$

while on the oxide surface the velocity is unknown and the pressure is in equilibrium with the ambient pressure or with the pressure of the nitride layer. At the nitride boundary we calculate the pressure through beam bending theory.

Equations (11) and (12) are solved by the artificial compressibility method [11], [14]. The problem of missing boundary condition for V on the oxide surface is eliminated by imposing an extra

$$\frac{dV}{dn} = 0 \quad (14)$$

boundary condition on the surface [15].

An example of two-dimensional oxidation is shown in Fig. 7. Fig. 7a. shows the calculated oxide shape and equiconcentration lines of the oxidant. In Fig. 7b the velocity of the oxide elements is shown.

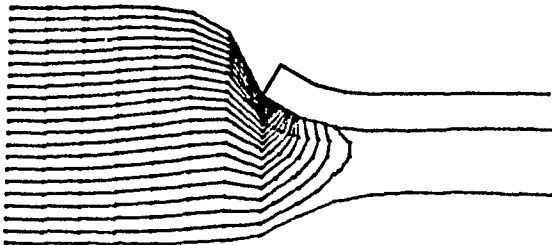


Fig. 7a. Bird's beak shape and oxidant distribution obtained by 2D oxidation model

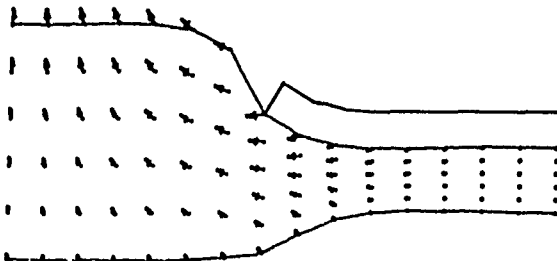


Fig. 7b. Velocity distribution of the oxide elements.

IMPLANTATION

The ion implantation model of APT allows several layers and masks of complicated shape. The only assumption we make that the layers can substitute each other with an appropriate choice of the substitute. The width of the substitute is calculated numerically assuming a longitudinal Pearson IV distribution. For shaped layers the total ion beam is subdivided into parallel elementary beams and the above technique is used for each elementary cross section with a Gaussian lateral distribution. The resulting distribution is determined by numerical integration. For the two-dimensional case the elementary lateral Gaussian distribution is one-dimensional, for the three-dimensional case a two-dimensional Gaussian lateral distribution is used for each elementary beam.

The dopant distribution for the 2D case can be calculated as follows,

$$C(z, x) = \frac{1}{\sqrt{2\pi} \Delta R_{pLAT}} \int_{-\infty}^{+\infty} N(z, x') \exp\left(-\frac{(x-x')^2}{2 \Delta R_{pLAT}^2}\right) dx' \quad (15)$$

where z and x are longitudinal and lateral coordinates respectively. $N(z, x)$ is calculated numerically for every x . For a given x in the i -th layer:

$$N_i(z, x) = F_i(z - z_i + \xi_i) \quad z_i < z < z_{i+1} \quad (16)$$

where F is the distribution is the homogenous target. The ξ_i displacement is computed solving the equation:

$$\xi_1 = 0, \quad \xi_i = \int_0^{\xi_i} F_i(z) dz = \sum_{j=i}^{i-1} Q_j \quad i > 1 \quad (17)$$

where Q is the total number of impurity atoms implanted into the j -th layer.

ETCHING AND DEPOSITION

APT allows up to 10 covering layers on the silicon surface. Every layer is defined by the nodes of a broken line approximating the profile of the layer. Etching or deposition results in the successive displacement of the broken line. During every step a number of new nodes are generated for a more accurate profile description. To avoid an extreme increase of the computation time following every time step the

unnecessary nodes are deleted at places with higher radius of curvature. Every line passes the simulated area from the beginning to the end even if the layer represented by the line is missing in some regions. In these regions the nodes of the layer with zero thickness have to coincide with the respective nodes of the underlying layer, otherwise the layer structure degenerates due to the rounding errors.

APT can simulate wet and reactive ion etching at present. Fig. 8. shows an example of wet etching.

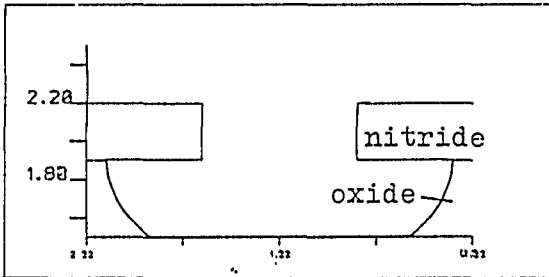


Fig. 8. Wet etching of SiO₂ through nitride window.

The deposition model takes three different physical mechanism into account [10]. They differ in the local deposition rate dependence of the angle of incidence. They are called "isotropic", "cosine", and "cosine squared" cases respectively, and are shown in Fig. 9.

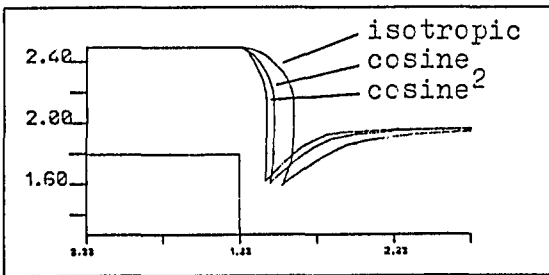


Fig. 9. Deposition models of APT

When performing a deposition step, the model combines the above three cases according to the technological conditions. Deposition of a sputtered layer over reactive ion etched silicon oxide structure is shown in Fig. 10.

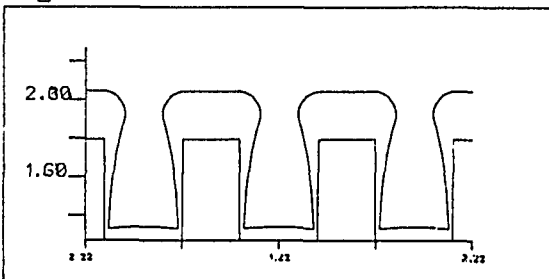


Fig. 10. Deposition of a layer with sputtering.

EXAMPLES

In this section the capabilities of APT are illustrated by the simulation of different steps of NMOS technology.

In the example shown below three sequential steps of the NMOS technology have been simulated by APT.

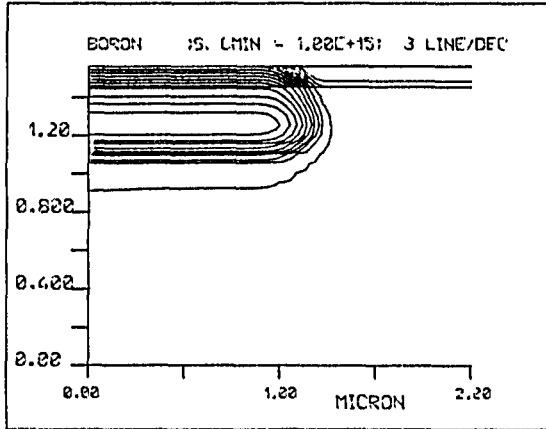


Fig. 11. Field area after field implantation.

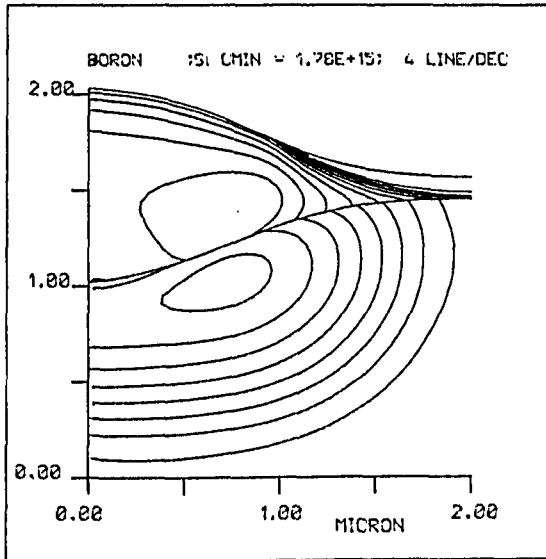


Fig. 12. Boron distribution in the Si and SiO₂ after local oxidation.

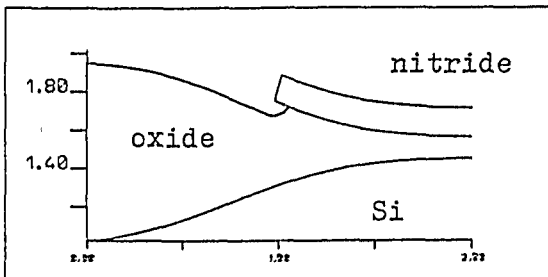


Fig. 13. Layer shape after 100 nm oxide etching.

The following figures show some typical final distributions of NMOS technology in different cross sections.

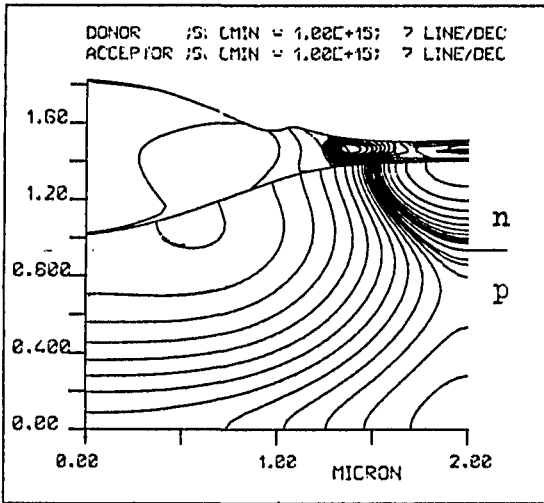


Fig. 14. Distribution of B and P in the field area and the depletion channel.

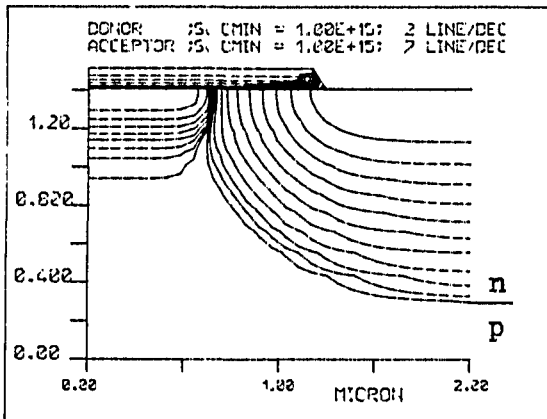


Fig. 15. Dopant distribution in the enhancement channel-source area

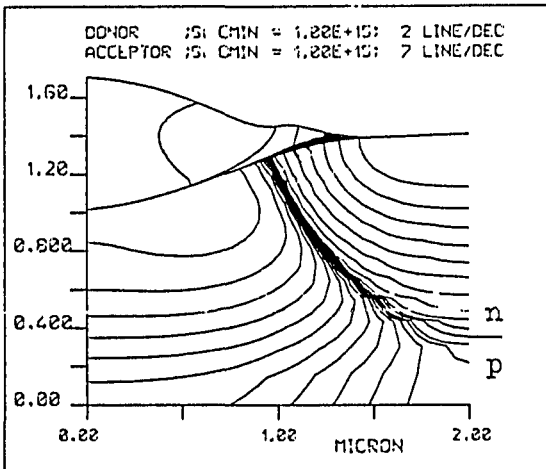


Fig. 16. Final distribution in the field-source region.

The following figures show the perspective view of the same distributions as Figs. 14 to 16.

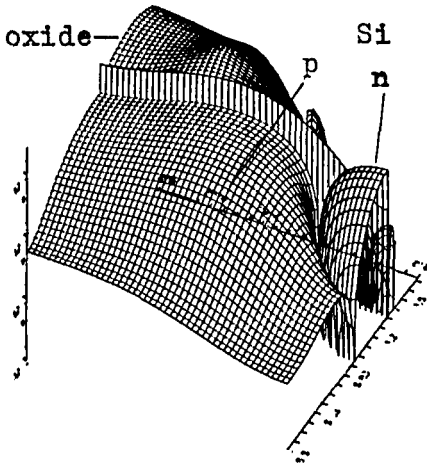


Fig. 17. Distribution of B and P in the field area and the depletion channel.

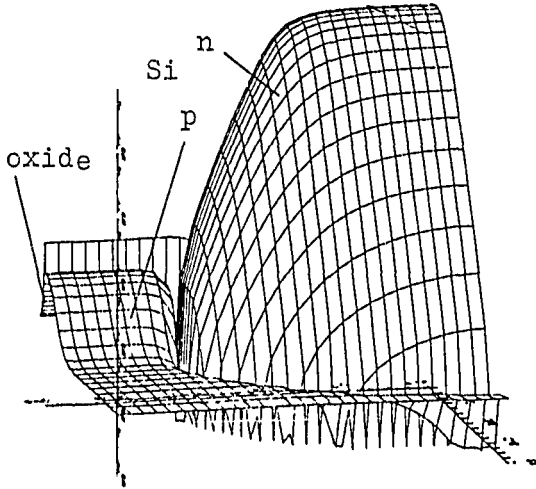


Fig. 18. Dopant distribution in the enhancement channel-source area.

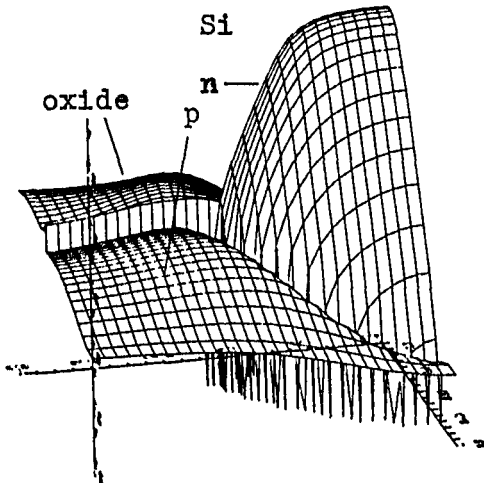


Fig. 19. Final distribution in the field-source region.

REFERENCES

1. Koltai, M. - Trutz, S. - Lazar, L.
"Two and Three Dimensional Semiconductor Technology Simulation"
Proceedings of 13th Yugoslav Conference on Microelectronics, p.337, 1985.
2. Stone, H.L.
"Iterative Solution of Implicit Approximations of Multidimensional Partial Differential Equations"
SIAM J. Num.An., Vol. 5, p.530, 1968.
3. Grove, A.S. et al.
"Redistribution of Impurities during Thermal Oxidation of Silicon"
J. Appl. Phys., Vol. 35, p.2695, 1964.
4. Penumalli, B.R.
"Two-Dimensional Simulation Program, BICEPS"
IEEE Trans. ED-30, p.986, 1983.
5. Av-Ron, M. et al.
"Distribution of dopant in SiO₂-Si"
J. Appl. Phys., Vol. 47, p.3159, 1976.
6. Lynch, D.R. et al.
"Finite Elements for the Solution of Parabolic Problems"
Int. J. Num. Meth., Vol. 17, p.81, 1981.
7. Fair, R.B.
"Proc. of Third Int. Symp. on Silicon Materials Sci. and Techn."
The El. Chem. Soc. 1977.
8. Fair, R.B. and Tsai, J.C.C.
"Quantitative Model for the Diffusion of Phosphorous"
J. El. Chem. Soc., Vol. 124, p.1107, 1977.
9. Koltai, M. and Trutz, S.
"Two and three-Dimensional Simulation of LSI Fabrication Process"
Proc. Microelectronics'84, Praha.
10. Allen, R.W.
"The Modelling of Sputtering and Etching"
Proc. of the Int. Conf. on Simulation of the Semiconductor Devices and Process., Swansea, 1984.

11. Daeje Chin and Dutton, R.W.
"A General Solution Method for Two-Dimensional
Nonplanar Oxidation"
IEEE Trans. ED-30, p.993, 1983.
12. Thye-Lai Tung and Antoniadis, D.A.
"A Boundary Integral Equation Approach to Oxidation
Modelling"
IEEE Trans. ED-32, p.1954, 1985.
13. Poncet, A.
"Finite-Element Simulation of Local Oxidation of
Silicon"
IEEE Trans. CAD-4, p.41, 1985.
14. Chorin, A.B.
"Numerical Solution of the Navier-Stokes Equations"
J. of Comp. Phys., Vol. 22, p.745, 1968.
15. Chu, C.K. and Sereny, A.
"Boundary Condition in Finite Difference Fluid
Dynamic Codes"
J. of Comp. Phys., Vol. 15, p.476, 1974.
16. Wilson, A.L.
"Numerical Solution of the Quasilinear Poisson
Equation"
J. of Comp. Physics, Vol. 2, p.149, 1967.